Journal of Marine Science and Technology

Volume 23 | Issue 4 Article 19

MODLING OF UPPER OCEAN HEAT BUDGET VARIATIONS IN RESPONSE TO THE PASSAGE OF SUPER TYPHOON SINLAKU (2008) IN THE WESTERN NORTH PACIFIC

Zhe-Wen Zheng
Institute of Marine Environmental Science and Technology and Department of Earth Science, National Taiwan Normal University, Taipei, Taiwan, zwz@ntnu.edu.tw

Nan-Jung Kuo
Department of Marine Environmental Informatics, National Taiwan Ocean University, Keelung, Taiwan

Quanan Zheng
Department of Atmospheric and Oceanic Science, University of Maryland, College Park, Maryland, USA.

Ganesh Gopalakrishnan
Scripps Institution of Oceanography, University of California San Diego, La Jolla, California, USA.

MODLING OF UPPER OCEAN HEAT BUDGET VARIATIONS IN RESPONSE TO THE PASSAGE OF SUPER TYPHOON SINLAKU (2008) IN THE WESTERN NORTH PACIFIC

Acknowledgements

The authors deeply appreciate three anonymous reviewers and executive editor of JMST. Their valuable comments and suggestions largely improve the presentation of this manuscript. Thanks also go to Dr. Sang-Ki Lee of RSMAS/CIMAS for sharing thoughtful idea of heat-budget computation. The TMI/AMSR-E SST data were provided by Remote Sensing Systems. GFS parameters were provided by NCDC and altimeter products were provided by AVISO with support from CNES. ECMWF/QuikSCAT blended winds were derived from French Research Institute for Exploitation of the Sea (ifremer). This work was supported by the National Science Council of Taiwan through grant NSC 100-2119-M-003-006, as well as partially supported by the U. S. NOAA/NESDIS Ocean Remote Sensing Funding Program 05-01-11-000, and the U. S. NSF Program AGS-1061998 (Q. Zheng).

Journal of Marine Science and Technology, Vol. 23, No. 4, pp. 551-557 (2015)
DOI: 10.6119/JMST-013-0909-6

MODLING OF UPPER OCEAN HEAT BUDGET VARIATIONS IN RESPONSE TO THE PASSAGE OF SUPER TYPHOON SINLAKU (2008) IN THE WESTERN NORTH PACIFIC

Zhe-Wen Zheng[1], Nan-Jung Kuo[2], Quanan Zheng[3], and Ganesh Gopalakrishnan[4]

Key words: numerical modeling, air-sea interaction, Regional Ocean Modeling System, typhoons.

ABSTRACT

In 2008, Super Typhoon Sinlaku (2008) passed over a pre-existing cyclonic eddy (PCE) in the western North Pacific, causing an extreme cooling response at 22.5°N, 125°E. This case provides a rare opportunity to explore the physical mechanisms that trigger an extreme cooling response to a typhoon underlying the influence of PCEs. In this study, cooling response to Sinlaku was observed by TMI/AMSR-E microwave SSTs and simulated using the Regional Ocean Modeling System. To elucidate the impact of a PCE, in addition to standard run (EXP_{std}), another experiment that eliminates the influence of a PCE (EXP_{nonPCE}) was designed and executed. By conducting upper ocean heat budget analysis on modeling diagnostic outputs, it is found that PCE enhances the cooling response by enhancing both the entrainment and upwelling simultaneously; but the dominant terms balancing the heat budget were not greatly altered by the PCE. Finally, the vertical thermal gradient is shown to be the essential factor boosting the enhancement of entrainment and upwelling, thus cooling the upper ocean.

I. INTRODUCTION

An upper ocean cooling response to a tropical cyclone is a key process occurring in the interface between the lower atmosphere and the upper ocean, because of its potential to modify typhoon intensity through energy exchange (Chang and Anthes, 1979; Black and Holland, 1995; Schade and Emanuel, 1999). For long, the upper ocean response induced by tropical cyclones has attracted substantial attention from researchers in both atmospheric and oceanic fields. Previous studies have suggested that the response of the ocean to typhoons and hurricanes depends not only on the speed and size of the storm but also on the properties of the underlying ocean (Price, 1981; Wentz et al., 2000; Lin et al., 2003; Walker et al., 2005; Zheng et al., 2008; D'Asaro et al., 2011).

Generally, the impact of preexisting upper ocean conditions on the cooling process has two types. First, a warm oceanic eddy preexisting on the pass track of a typhoon acts as an insulator between typhoons and the cold water of the deeper ocean, thus suppressing the cooling response to a certain typhoon (Hong et al., 2000; Shay et al., 2000; Lin et al., 2008; Lin et al., 2009). Second, while a typhoon encountering a pre-existing cyclonic eddy (PCE), it shows a contrary scenario that the PCE significantly enhances the efficiency of typhoon-caused surface cooling in the upper ocean (Walker et al., 2005; Prasad and Hogan, 2007; Zheng et al., 2008; Zheng et al., 2010b). This process has the potential to reduce the energy fed into the storm from the ocean because evaporation and conduction directly depend on the air-sea temperature difference (Leipper and Volgenau, 1972). All of these processes are crucial for typhoon and hurricane intensity change prediction, because an upper ocean response to a typhoon is closely associated with energy transferring across the air-sea interface, thus changing subsequent typhoon and hurricane intensity changes (Leipper and Volgenau, 1972; Black and Holland, 1995; Schade and Emanuel, 1999).

Previous studies have largely improved understanding of the relationship between pre-existing oceanic conditions and the subsequent cooling process of a typhoon. Nevertheless, some critical concerns have not been sufficiently clarified. For instance, (1) the physical mechanisms that trigger the extreme cooling response to a typhoon underlying the influence of

Paper submitted 06/21/13; revised 08/27/13; accepted 09/09/13. Author for correspondence: Zhe-Wen Zheng (e-mail: zwz@ntnu.edu.tw).
[1] Institute of Marine Environmental Science and Technology and Department of Earth Science, National Taiwan Normal University, Taipei, Taiwan, R.O.C.
[2] Department of Marine Environmental Informatics, National Taiwan Ocean University, Keelung, Taiwan, R.O.C.
[3] Department of Atmospheric and Oceanic Science, University of Maryland, College Park, Maryland, USA.
[4] Scripps Institution of Oceanography, University of California San Diego, La Jolla, California, USA.

PCEs. Although entrainment is generally considered the key mechanism that dominates the mixed layer cooling to a tropical cyclone in a regular case (Price, 1981; Jacob et al., 2000), it is worth noting that the dominant mechanism to a cooling response may change underlying various background conditions (e.g., Typhoon Kai-Tak in Lin et al., 2003). Therefore, question remains whether the influence of PCE and entrainment still play crucial roles in the cooling process. (2) The process of how the PCE modifies the upper ocean heat budget underlying a typhoon passage has not been resolved in previous studies.

Sinlaku (2008) was a Category 4 super typhoon that formed nearly 300 km east of Luzon Island on September 8, 2008, and then moved northward towards Taiwan. Finally, it made landfall on the northeastern coast of Taiwan on September 12, 2008. During its passage, Sinlaku passed over a pronounced PCE near 22.5°N, 125°E and caused an extreme cooling response (of more than 5°C). This PCE was a westward propagated mesoscale eddy. It appeared within the study area since the 20th of August. Therefore, Sinlaku provided a rare opportunity for clarifying the aforementioned issues.

This study analyzed the upper ocean heat budget to elucidate the physical processes contributing to temperature variations during the typhoon passage. Thus, the dominant mechanisms triggering the extreme cooling to Sinlaku were found. Meanwhile, by comparing the modeling results using standard experiment and control experiment, the role that the PCE plays on the upper ocean heat budget is elucidated. Finally, model simulated 3-D velocity components, diffusion coefficient, and vertical temperature gradient were analyzed to demonstrate how the PCE enhanced the cooling response.

II. METHODOLOGY

1. Model Descriptions and Experiments Design

The Regional Ocean Modeling System (ROMS) used in this work is a free-surface, primitive equation, terrain-following oceanic model, in which barotropic and baroclinic momentum equations are resolved separately, where short time steps are used to advance the surface elevation and barotropic momentum equations and a much longer time step are used to compute temperature, salinity, as well as baroclinic momentum. A special two-way time-averaging procedure was employed for the barotropical mode in ROMS, whereas a third-order accurate predictor (Leap-Frog) and corrector (Adams-Molton) time-stepping scheme was used to discretize the baroclinic mode. The combination of these schemes implemented in ROMS enables the generation of steep gradients, and effective resolution for a given grid (Shchepetkin and McWilliams, 1998). Finally, a non-local, K-Profile Parameterization (KPP) boundary-layer scheme was used to parameterize the sub-grid scale vertical mixing processes in ROMS. Further description and validation of this model can be seen in Shchepetkin and McWilliams (1998; 2003).

In this study, the model domain covers the partial western North Pacific, the continental shelf of the East China Sea, and the northern South China Sea (see Fig. 1). Model bathymetry is derived from ETOP02 bottom topography (Smith and Sandwell, 1997). The model has a horizontal resolution of 1/8° (~12 km). Vertically, 32 s-coordinate levels are unevenly distributed for a favorable resolution of the upper ocean. The advantage of choosing such a complex vertical coordinate system is to provide an appropriate vertical resolution in the upper ocean, and save the computation cost.

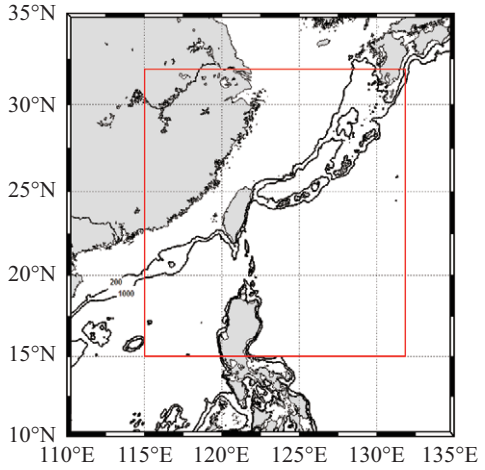

Fig. 1. Model domain (red rectangle, 15-32°N, 115-132°E) in this study, covering partial western North Pacific, continental shelf of the East China Sea, and the northern South China Sea.

The model is forced both by mechanical and thermal forcing. Parameters including 2 m and surface air temperature, 2 m atmospheric relative humidity, downward shortwave and longwave radiation fluxes, and precipitation rate from Global Forecast System (GFS) (available at http://nomads.ncdc.noaa.gov/) are used to estimate heat exchange fluxes across the sea interface. Six-hourly 0.25° ECMWF/QuikSCAT blended wind, obtained from French Research Institute for Exploitation of the Sea (IFREMER) through website ftp://ftp.ifremer.fr/, is used to force the model for its appropriately spatial resolution and temporal coverage, the resolving ability of this wind product can be seen in previous study (Zheng et al., 2010a). These fluxes are generated during the model run, instead of directly prescribing them in the experiments.

The initial and lateral conditions used in the model are derived from the HYCOM/NCODA Global 1/12° analysis field. All modeling experiments were configured based on a diagnostic frame. This product uses the Navy Coupled Ocean Data Assimilation (NCODA) system (Cummings, 2005) for data assimilation. Assimilated variables include satellite altimeter observations, satellite and in situ SST, as well as available in-situ vertical temperature and salinity profiles from Argo floats, gliders, and moored buoys. Additional details about the cooperation of HYCOM/NCODA outputs and ROMS can be seen in Zheng et al. (2010a; 2010b).

To evaluate the impacts of PCE, in addition to the standard experiment (EXP_{std}), we further conduct another run

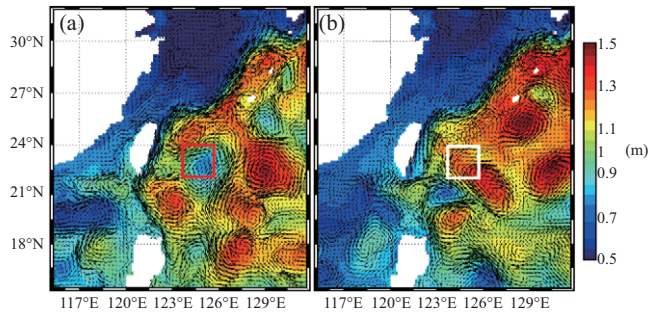

Fig. 2. Initial conditions derived from HYCOM/NCODA analysis for (a) EXP_{std} and (b) EXP_{nonPCE}. Color boxes in both figures denoted the areas used for heat budget analysis.

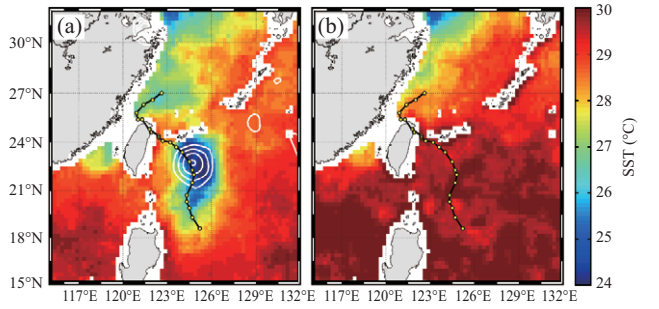

Fig. 3. (a) TMI/AMSR-E observed maximum cooling responses during typhoon Sinlaku passage (September 10-18, 2008). The SSHA contours of the PCE are superimposed on the maximum SST drop images. (b) TMI/AMSR-E observed SST on September 9, 2008. Moving tracks of Sinlaku are marked by yellow dots. The beginning time of the track is 12:00 on September 9, 2008. The temporal interval of each dot is 6 hours.

(EXP_{nonPCE}) with the same configurations as in standard experiment but with different initial conditions. The initial conditions in EXP_{nonPCE} are also derived from HYCOM/NCODA system, except for that on September 8, 2007. Fig. 2 shows the initial conditions, including the sea surface height and the surface current vector derived from HYCOM/NCODA products on September 8, 2008 (Fig. 2(a)) and September 8, 2007 (Fig. 2(b)), for standard experiment (EXP_{std}) and non-PCE experiment (EXP_{nonPCE}). Compared both figures, one can see that, relative to the existence of an unusually intense cyclonic eddy on September 8, 2008, EXP_{nonPCE} can serve as a climatological background without the influence of a pronounced PCE.

2. Satellite Observations

Here, merged SST products retrieved from Tropical Rainfall Measuring Mission (TRMM) Microwave Imager (TMI) and the Advanced Microwave Scanning Radiometer for EOS (AMSR-E) onboard the Aqua satellite are used to quantify the cooling response to Sinlaku (Wentz et al., 2000). The product has a daily temporal resolution and a 0.25 degree spatial resolution. The preexisting cyclonic eddy is characterized by a negative sea surface height anomaly (SSHA) merged from Jason-2 and ENVISAT satellites (Lin et al., 2005; Lin et al., 2008; Zheng et al., 2008). The SSHA product with a 0.25° spatial resolution and a 7-day temporal interval is provided by Archiving Validation and Interpretation of Satellite Data in Oceanography (AVISO).

III. SURFACE COOLING IN RESPONSE TO SINLAKU'S PASSAGE

In this section, we examine the relationship between PCE prior to Sinlaku passage and the enhanced surface cooling induced by Sinlaku after its passage. Fig. 3(a) shows the maximal cooling response induced by Sinlaku during its passage. The maximal cooling response is estimated by a series of TMI/AMSR-E satellite-observed SST drops (relative to SST prior to Sinlaku's passage, as shown in Fig. 3(b)) caused by Sinlaku along its track. The negative SSHA (white contours in Fig. 3(a)) on September 10, 2008 are superimposed on the

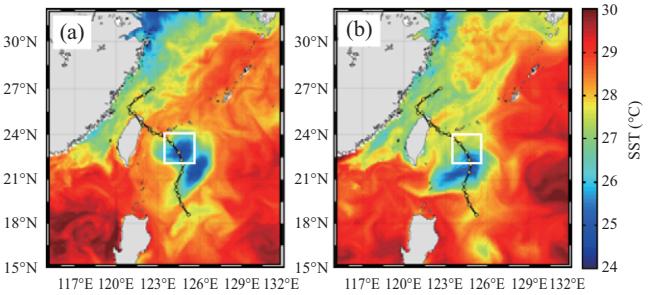

Fig. 4. ROMS simulated maximum cooling responses during typhoon Sinlaku passage from (a) standard experiment (EXP_{std}), and (b) model run with eliminated influence of PCE (EXP_{nonPCE}). White boxes represent the area used for heat budget computation.

cooling response. Comparing the cooling response to the location of PCE characterized by negative SSHA, it is evident that the extreme surface cooling response caused by Sinlaku seems to be highly associated with the existing PCE prior to Sinlaku's passage. This relationship is generally consistent with previous studies (e.g., Walker et al., 2005; Zheng et al., 2008) but is much more evident. This indicates that Sinlaku provided a rare case for elucidating the role of PCE play in modulating upper ocean heat budget variations during a typhoon passage.

Figs. 4(a) and 4(b) show the results simulated using EXP_{std} and EXP_{nonPCE}. Comparing the simulated cooling responses in both experiments to those observed by TMI/AMSR-E, the results simulated in EXP_{std} obviously fit the satellite observations much more favorably than those simulated using EXP_{nonPCE}. Both the central location and the magnitude of the maximal cooling simulated by EXP_{std} agree reasonably well with those characteristics retrieved from satellite observations. Meanwhile, as expected, the results derived from EXP_{nonPCE} do not agree with satellite observations well. This implies that, with the synergy of proper upper ocean conditions (e.g. the use of real-time HYCOM/NCODA output fields as initial

conditions of ROMS), ROMS has the potential to generally reproduce the upper ocean heat budget variations and thus the surface cooling in response to a typhoon passage.

IV. HEAT BUDGET VARIATIONS DURING SINLAKU PASSAGE

Here, the terms balancing the heat budget equation (refer to Lee et al. (2007)) are computed based on model diagnostic outputs. The physical processes affecting the upper ocean temperature are thus elucidated. The equation has the form as

$$Q_T = Q_{U+V} + Q_W + Q_S + Q_{DV} + Q_{DH}, \quad (1)$$

where Q_T is the total temperature change rate at a certain depth, Q_{U+V}, Q_W, Q_S, Q_{DV}, and Q_{DH} are the temperature change rates contributed by horizontal advection, vertical advection, surface heat flux, vertical diffusion, and horizontal diffusion, respectively. Because the horizontal heat flux divergence is largely compensated by the vertical heat flux convergence, the individual vertical and horizontal advection terms are combined into a single term, total advection Q_{ADV}. In addition, because the horizontal diffusion term Q_{DH} is negligibly small, it is not shown in this analysis. According to the average September temperature profiles from the World Ocean Atlas 2001 (WOA01) in Stephens et al. (2002), five depths, 10 m, 15 m, 25 m, 30 m, and 40 m, were selected to represent temperature variations from the mixed-layer, to the mixed-layer base, and to the upper part of thermocline. Heat budget terms were averaged within a box area of 2° by 2° centered at 23°N, 124.75°E, as depicted in Fig. 4.

1. Heat Budget Variations in Standard Experiment (EXP_{std})

Figs. 5(a)-5(e) show the heat budget variations simulated using EXP_{std}. In addition to the heat budget within mixed-layer (Fig. 5(a)), the heat budget terms below the mixed-layer (Figs. 5(c)-5(e)) are also presented to elucidate the underlying processes causing subsurface temperature changes. For clarity, the y-axis in Figs. 5(a)-5(e) has the same scale. Comparing these heat variations within different depths, clearly, different processes dominate the evolutions of heat budget terms at various depths. Vertical mixing dominates the heat variations within the mixed-layer, whereas advection plays a secondary role in the mixed-layer cooling during the passage of Sinlaku (see Figs. 5(a) and 5(b)). The heat variation at 25 m (Fig. 5(c)) shows a transitional scenario. At a depth of 40 m, advection becomes the dominant term in the heat-budget balance. The temperature change rate contributed by the surface heat flux is approximately 10% of the total thermal variations. This value is comparable to those suggested by previous studies (Price, 1981; Jacob et al., 2000).

During the typhoon passage, vertical mixing contributed a net warming at a depth of 30 m during September 11-12. This

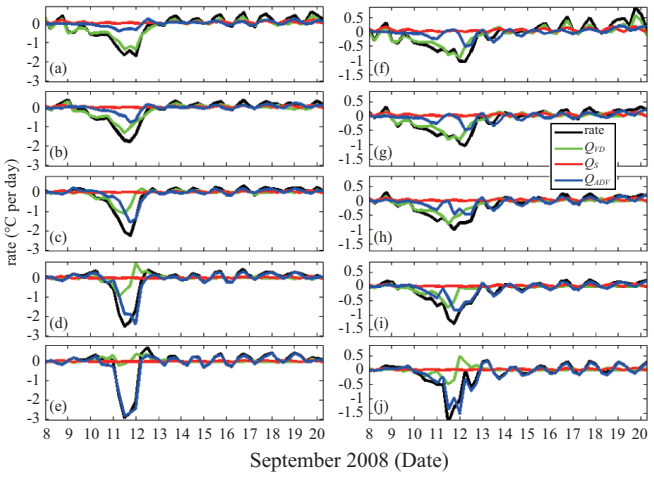

Fig. 5. Area-averaged heat budget terms computed using the results simulated by EXP_{std} in °C per day at five depths (a) 10 m, (b) 15 m, (c) 25 m, (d) 30 m, and (e) 40 m. (f)-(j) are the same as (a)-(e), except for results simulated using EXP_{nonPCE} at corresponding depths. The heat budget terms include the temperature change rate (Q_T), temperature change rates contributed by surface heat flux (Q_S), vertical diffusion (Q_{VD}) and total advection (Q_{ADV}).

warming was attributed to mixed-layer deepening caused by entrainment mixing, as shown in Price (1981). Another distinct feature revealed in the heat variations is the periodical oscillation occurring after the passage of Sinlaku on September 12. Using the Fast Fourier Transform analysis, we determine the oscillation period as approximately 27.3 hours. This period is close to the local inertial period (30.7 hours). The 11% period difference is considered to be associated with the blue-shift by the pressure gradient as noted in Sanford et al. (2007).

2. Heat Budget Variations in Control Experiments (EXP_{nonPCE})

Figs. 5(f)-5(j) show the heat budget variations simulated in EXP_{nonPCE}. It is worth to note that the scales of y-axis in Figs. 5(f)-5(j) are about half of those scales using in Figs. 5(a)-5(e). In other words, the cooling responses simulated using EXP_{nonPCE} are much smaller than those simulated using EXP_{std}. Comparing both experiments elucidates the effects of the PCE. This implies that the PCE plays a crucial role in enhancing upper layer cooling. However, more interesting is that, despite the obviously different magnitudes in both experiments, heat budget terms in both experiments show similar evolved process. For instance, both of them reveal a near-inertial oscillation with a period of approximately 27 hours after the passage of Sinlaku. In addition, the variations within and below the mixed-layer are also dominated by entrainment and advection, respectively.

In short, the PCE modifies both the strength of temperature changes through the vertical mixing and the advection simultaneously. However, the dominant terms balancing the heat budget were not greatly altered by the PCE.

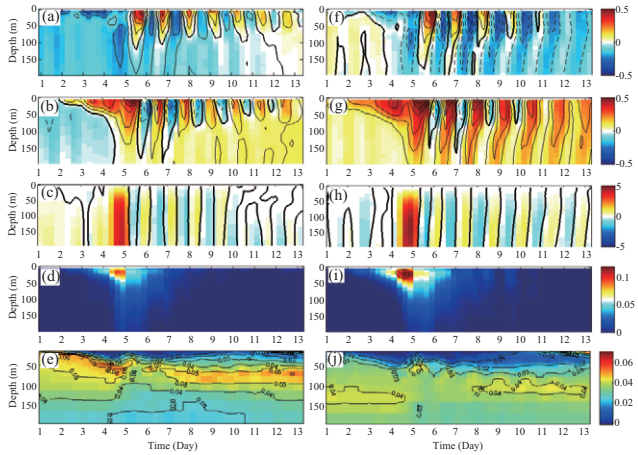

Fig. 6. Model simulated continuous profiles of (a) the velocity u-component (ms^{-1}), (b) v-component (ms^{-1}), (c) and vertical component (10^{-5} ms^{-1}), (d) vertical diffusion coefficient (*AKt* in m^2 s^{-1}), and (e) vertical temperature gradient (°C m^{-1}) in EXP_{std}. Those values were averaged over a two degree box area centered at 23°N, 124.75°E. (f)-(j) are the same as (a)-(e), except for that derived from EXP_{nonPCE}.

3. How the PCE Modifies the Upper Ocean Heat Budget during a Typhoon Passage?

In this section, essential parameters including, velocity components in three dimension, vertical diffusion coefficient, and vertical temperature gradient were integrated and analyzed to resolve how the PCE modified the upper ocean heat budget and thus the cooling response to Sinlaku. Generally, the enhancement of temperature changes in the upper ocean may be due to the strengthening of entrainment and upwelling and the upper ocean stratification; that is, a thinner mixed-layer depth (MLD) and sharper vertical temperature gradient. Figs. 6(a)-6(c) show the continuous profiles of velocity fields (*u*, *v*, *w*). Figs. 6(d) and 6(e) show vertical diffusion coefficient (*AKt* in m^2 s^{-1}), and vertical temperature gradient (°C m^{-1}) averaged from a box area centered at 23°N 124.75°E (white box in Fig. 4) from EXP_{std}. Figs. 6(f)-6(j) are the same as Figs. 6(a)-6(e), except for that from EXP_{nonPCE}. All these terms are associated with the rate of the upper ocean cooling in both experiments.

In ROMS, the vertical mixing (entrainment) term has the form of $\frac{\partial}{\partial\sigma}\left(\frac{AKt}{H_z \cdot mn}\frac{\partial\phi}{\partial\sigma}\right)$ where ϕ represents one of *u*, *v*, temperature or salinity, *AKt* denotes the corresponding vertical diffusion coefficient, and H_z, *m*, *n*, and σ are derivatives resulting from the transformation of the z-coordinate to the s-coordinate (Song and Haidvogel, 1994). Refer to the vertical mixing term in ROMS, enhanced temperature response in the upper ocean contributed by vertical mixing may be due to enhancement of *AKt* and/or the increase of vertical temperature gradient. On the other hand, temperature changes caused by advection are mainly contributed by the strengths of upwelling and the vertical temperature gradient.

Figs. 6(a)-6(d) and Figs. 6(f)-6(i) show that the dynamic fields (*u*, *v*, *w* and *AKt*) derived from EXP_{std} and EXP_{nonPCE} are quite similar. In both experiments, the upper layer velocity demonstrates a clockwise-rotating inertial motion (Figs. 6(a), 6(b), 6(f), and 6(g)). This is attributed to the resonance of wind stress vector rotating clockwise on the right side of the track with inertial motions (Price, 1981; Sanford et al., 2007). The divergence of the upper layer horizontal velocity field causes upwelling and downwelling with a near-inertial period (see Figs. 6(c) and 6(h)), termed inertial pumping. Concurrently, the vertical velocity and vertical diffusion coefficient (which are used to reflect the strengths of upwelling and vertical mixing) in EXP_{nonPCE} are even slightly larger than those in EXP_{std}. Recall the much stronger upper ocean response of EXP_{std} shown in the heat budget analysis (seeing Fig. 5). This result implies that the non-dynamic term (e.g. vertical temperature gradient) may play a key role in modulating the upper ocean heat budget during a typhoon passage underlying the influence of PCE.

Figs. 6(e) and 6(j) show the vertical temperature gradient (°C m^{-1}) in EXP_{std} and EXP_{nonPCE}, respectively. The minimal gradient area (blue shade) can approximately be treated as the distribution of mixed-layer. According to the variations of MLD, in the forced period, the MLD is gradually deepened by the entrainment. Immediately, the enhanced upwelling makes the MLD become shallow by pumping cold water upward form the subsurface and overwhelms the mixed-layer deepening caused by the entrainment. Finally, with the decrease of entrainment and upwelling, near-inertial oscillations gradually dominate the MLD variability in the relaxation period (see Figs. 6(e) and 6(j)). In addition to the MLD variability, the vertical temperature gradient was somewhat different in both experiments. In EXP_{std}, the temperature gradient just below the mixed-layer varies drastically, in contrast to the gentle variations of vertical temperature gradient in EXP_{nonPCE}. Because of the large differences in upper ocean thermal stratification, the typhoon passage can cause the upper ocean cooling with different magnitudes through entrainment and upwelling under identical wind-forcing. In other words, the sharper vertical temperature gradient is the crucial factor causing the upper ocean heat budget changes and thus enhancing the cooling response, underlying the influence of PCE, rather than the differences of dynamic fields between both experiments.

V. CONCLUSIONS

Super Typhoon Sinlaku 2008 passing directly over a huge cyclonic eddy at 23°N, 124.5°E provided a great opportunity for exploring some key issues that have not been sufficiently clarified. To approach these scientific issues, ROMS is used to reproduce the upper ocean response to the passage of Super Typhoon Sinlaku. Model simulated upper ocean cooling generally agrees favorably with the response observed by satellite microwave sensors.

Subsequently, by comparing the model results from the

standard experiment and control run, we examined the sensitivity of the upper ocean cooling response to PCE. Although the difference between both experiments cannot totally be attributed to the contributions of cyclonic eddy only, because initial and boundary conditions using in both experiments were derived from real oceanic environment. However, it is noted that the specific goal of this analysis is to reveal the impact of a cyclonic eddy on the whole thermal evolution relative to a normal case (without the influence of PCE). That's why we use another real oceanic environment (derived from HYCOM/NOCDA outputs on 8 September 2007) as initial and boundary conditions in EXP_{nonPCE} rather than applying a fully ideal experiment. Therefore, though the difference between both experiments didn't totally equate to the contribution of cyclonic eddy, it is believed that this might not cause adversely effects on the demonstration of the impact of PCE to the upper ocean heat budget during a typhoon passage.

In addition, the terms balancing the temperature equation were computed, and the physical mechanisms dominating the upper ocean heat budget during a typhoon passage at different depths were quantified. The results of heat budget analyses show that the vertical mixing (entrainment) dominates the mixed-layer heat variations; whereas the advection dominates the temperature changes below the mixed-layer. Comparing the heat budgets from EXP_{std} and EXP_{nonPCE} suggests that the PCE enhances the upper ocean cooling response by increasing the contributions of advection and vertical mixing simultaneously. Nevertheless, it is worth noting that the balance of the upper ocean heat budget was not dramatically altered by the PCE.

Finally, by comparing the time-series profiles of dynamic fields to vertical thermal stratification evolutions during the typhoon passage, it is found that the different rate of cooling within the mixed-layer can be mainly attributed to the differences of the pre-storm vertical temperature gradient. Namely, sharper thermal stratification in the upper ocean accompanying the PCE enhances the efficiency of the upper ocean cooling through the entrainment and upwelling under identical wind-forcing and eventually the cooling response.

ACKNOWLEDGMENTS

The authors deeply appreciate three anonymous reviewers and executive editor of JMST. Their valuable comments and suggestions largely improve the presentation of this manuscript. Thanks also go to Dr. Sang-Ki Lee of RSMAS/CIMAS for sharing thoughtful idea of heat-budget computation. The TMI/AMSR-E SST data were provided by Remote Sensing Systems. GFS parameters were provided by NCDC and altimeter products were provided by AVISO with support from CNES. ECMWF/QuikSCAT blended winds were derived from French Research Institute for Exploitation of the Sea (ifremer). This work was supported by the National Science Council of Taiwan through grant NSC 100-2119-M-003-006, as well as partially supported by the U. S. NOAA/NESDIS Ocean Remote Sensing Funding Program 05-01-11-000, and the U. S. NSF Program AGS-1061998 (Q. Zheng).

REFERENCES

Black, P. G. and G. J. Holland (1995). The boundary layer of tropical Cyclone Kerry (1979). Monthly Weather Review 123, 2007-2028.

Chang, S. W. and R. A. Anthes (1979). The mutual response of the tropical cyclone and the ocean. Journal of Physical Oceanography 9, 128-135.

Cummings, J. A. (2005). Operational multivariate ocean data assimilation. Quarterly Journal of the Royal Meteorological Society 131, 3583-3604.

D'Asaro, E., P. Black, L. Centurioni, P. Harr, S. Jayne, I. Lin, C. Lee, J. Morzel, R. Mrvaljevic, P. P. Niiler, L. Rainville, T. Sanford and T. Tang (2011). Typhoon-ocean interaction in the western North Pacific: Part 1. Oceanography 24(4), 24-31.

Hong, X., S. W. Chang, S. Raman, L. K. Shay and R. Hodur (2000). The interaction between Hurricane Opal (1995) and a warm core ring in the Gulf of Mexico. Monthly Weather Review 128, 1347-1365.

Jacob, S. D., L. K. Shay and A. J. Mariano (2000). The 3D oceanic mixed layer response to Hurricane Gilbert. Journal of Physical Oceanography 30, 1407-1429.

Lee, S.-K., D. B. Enfield and C. Wang (2007). What drives seasonal onset and decay of the western hemisphere warm pool? Journal of Climate 20(10), 2133-2146.

Leipper, D. F. and D. Volgenau (1972). Hurricane heat potential of the Gulf of Mexico. Journal of Physical Oceanography 2, 218-224.

Lin, I.-I., W. T. Liu, C. Wu, G. T. F. Wong, C. Hu, Z. Chen, W. Liang, Y. Yang and K. Liu (2003). New evidence for enhanced ocean primary production triggered by tropical cyclone. Geophysical Research Letters 30(13), 1718, doi:10.1029/2003GL017141.

Lin, I.-I., I. F. Pun and C. C. Wu (2009). Upper-ocean thermal structure and the western North Pacific Category-5 typhoons. Part II: Dependence on translation speed. Monthly Weather Review 137, 3744-3757.

Lin, I.-I., C. C. Wu, K. A. Emanuel, I. H. Lee, C. R. Wu and I. F. Pun (2005). The Interaction of Supertyphoon Maemi (2003) with a warm ocean eddy. Monthly Weather Review 133, 2635-2649.

Lin, I.-I., C. C. Wu, I. F. Pun and D. S. Ko (2008). Upper-ocean thermal structure and the western North Pacific Category-5 typhoons. Part I: Ocean features and Category-5 typhoon's intensification. Monthly Weather Review 136, 3288-3306.

Prasad, T. G. and P. J. Hogan (2007). Upper-ocean response to Hurricane Ivan in a 1/25° nested Gulf of Mexico HYCOM. Journal of Geophysical Research 112, C04013, doi:10.1029/2006JC003695.

Price, J. F. (1981). Upper ocean response to a hurricane. Journal of Physical Oceanography 11, 153-175.

Sanford, T. B., J. F. Price, J. B. Girton and D. C. Webb (2007). Highly resolved observations and simulations of the ocean response to a hurricane. Geophysical Research Letters 34, L13604, doi:10.1029/2007GL029679.

Schade, L. R. and K. A. Emanuel (1999). The ocean's effect on the intensity of tropical cyclones: Results from a simple coupled atmosphere ocean model. Journal of the Atmospheric Sciences 56, 642-651.

Shay, L. K., G. J. Goni and P. G. Black (2000). Effects of a warm oceanic feature on Hurricane Opal. Monthly Weather Review 128, 1366-1383.

Shchepetkin, A. F. and J. C. McWilliams (1998). Quasi-monotone advection schemes based on explicit locally adaptive dissipation. Monthly Weather Review 126, 1541-1580.

Shchepetkin, A. F. and J. C. McWilliams (2003). Method for computing horizontal pressure-gradient force in an oceanic model with a nonaligned vertical coordinate. Journal of Geophysical Research 108(C3), 3090, doi:10.1029/2001JC001047.

Shchepetkin, A. F. and J. C. McWilliams (2005). The regional oceanic modeling system (ROMS): A split-explicit, free-surface, topography following-coordinate oceanic model. Ocean Modeling 9, 347-404.

Smith, W. H. F. and D. T. Sandwell (1997). Global seafloor topography from satellite altimetry and ship depth soundings. Science 277, 1957-1962.

Song, Y. and D. B. Haidvogel (1994). A semi-implicit ocean circulation model using a generalized topography-following coordinate system. Journal of Computational Physics 115(1), 228-244.

Stephens, C., J. I. Antonov, T. P. Boyer, M. E. Conkright, R. A. Locarnini, T. D. O'Brien and H. E. Garcia (2002). World Ocean Atlas 2001, vol. 1, Temperature. NOAA Atlas NESDIS. 49, NOAA, Silver Spring, Md.

Walker, N. D., R. R. Leben and S. Balasubramanian (2005). Hurricane forced upwelling and chlorophyll a enhancement within cold-core cyclones in the Gulf of Mexico. Geophysical Research Letters 32, L18610, doi: 10.1029/2005GL023716.

Wentz, F. J., C. Gentemann, D. Smith and D. Chelton (2000). Satellite measurements of sea surface temperature through clouds. Science 288, 847-850.

Zheng, Z.-W., C. R. Ho and N. J. Kuo (2008). Importance of pre-existing oceanic conditions to upper ocean response induced by Super Typhoon Hai-Tang. Geophysical Research Letters 35, L20603, doi:10.1029/2008GL035524.

Zheng, Z.-W., C. R. Ho, Q. Zheng, N. J. Kuo and Y. T. Lo (2010a). Satellite observation and model simulation of upper ocean biophysical response to Super Typhoon Nakri. Continental Shelf Research 30(13), 1450-1457.

Zheng, Z.-W., C. R. Ho, Q. Zheng, Y. T. Lo, N. J. Kuo and G. Gopalakrishnan (2010b). Effects of preexisting cyclonic eddies on upper ocean responses to Category 5 typhoons in the western North Pacific. Journal Geophysical Research 115, C09013, doi:10.1029/2009JC005562.